AIAA 2003-587

AIAA-2003-0587

Translational temperature measurement of arc-heater plumes by a laser absorption spectroscopy

Makoto MATSUI*, Satoshi OGAWA**, Kimiya KOMURASAKI †
and Yoshihiro ARAKAWA ‡
The university of Tokyo,
Hongo 7-3-1, Bunkyo, Tokyo 113-0033, Japan

Keywords: saturation, laser absorption spectroscopy, arc-heater, high enthalpy flow

Abstraction

Saturation phenomena in laser absorption spectroscopy applied to a glow discharge plasma and arc-heater plumes were examined. In a glow discharge tube, strongly saturated profiles of three ArI lines (840.82 nm, 842.46 nm and 852.14 nm) were observed, and the translational temperature was found to increase with laser intensity, which contradicts the inhomogeneous saturation theory. As for the arc-heater plumes, measured translational temperature differed depending on target absorption lines (ArI 840.82nm and OI 777.19 nm) though laser intensity is enough small to avoid absorption saturation.

Introduction

Arc-heaters are often used for the tests of Thermal Protection Systems of reentry vehicles. However, exact plume conditions are mostly unknown because they are usually in thermo-chemical nonequilibrium. Therefore, measurements of translational temperature in these high enthalpy flows will provide useful information for TPS researches.

In our previous research,[1)] translational temperature distributions in the university of Tokyo arc-heater plumes were measured by the laser absorption spectroscopy. As a result, the translational temperature deduced from the atomic oxygen line at 777.19 nm was different from that deduced from the argon line at 840.82 nm, as shown in Figs. 1 and 2. Moreover, these temperatures were also different from CFD result, as shown in Fig. 3. [2)]

* Graduate student, Department of Advanced Energy, Student Member AIAA, email: matsui@al.t.u-tokyo.ac.jp
** Graduate student, Department of Aeronautics and Astronautics
† Associate Professor, Department of Advanced Energy, Member AIAA,
‡ Professor, Department of Aeronautics and Astronautics, Member AIAA

The translational temperature should be independent of chemical species, because the energy relaxation time in the translational mode is much faster than the velocity of the flow. Therefore, there would be something to cause this discrepancy. In this study, the saturation phenomena were focused on and the influences of these phenomena on translational temperature measurements of a glow discharge tube and arc-heater plumes were investigated.

Theories of Line Broadening and Absorption Saturation

There are two types of broadening, that is, homogeneous broadening and inhomogeneous broadening. Homogeneous broadening consists of particles that are essentially equivalent and have the same transition energy while in inhomogeneous broadening, particles are distinguishable and reflect a distribution of their characteristics. As for the saturation phenomena, there is an important difference between these broadenings.

Homogeneous broadening

Homogeneous broadening is the combination of various broadenings such as natural broadening, pressure (Van der Waals) broadening and Stark broadening. These broadenings are all Lorentz type and each broadening is indistinguishable in real profiles.

In this case, absorption saturation is caused

by the population inversion with laser intensity. Absorption coefficient $k(\nu)$ at the incident laser intensity I is expressed as follows.

$$k(\nu) = k_0(\nu)\left[1 + \frac{I}{I_{\text{s\_homo}}(\nu)}\right]^{-1} \quad (1)$$

Here, $k_0(\nu)$ is unsaturated absorption coefficient and $I_{\text{s\_homo}}(\nu)$ is the saturation intensity of homogeneous broadening and expressed as follows.

$$I_{\text{s\_homo}}(\nu) = \frac{4\pi h\nu}{\phi\lambda^2}\frac{1}{g(\nu)} \quad (2)$$

Here, h is Plank constant, ν is the frequency, λ is the wavelength, g(ν) is the normalized line shape function, which is here a Lorentz distribution, and ϕ is defined as follows.

$$\phi = \frac{A_{ji}}{A_{ji} + Q} \quad (3)$$

Here, A_{ji} is the Einstein coefficient and Q is the quenching rate. Remarkable thing is that $I_{\text{s\_homo}}(\nu)$ depends on the line shape function g(ν). When the laser intensity is high, the line width is broadened as,

$$\Delta\nu_S = \Delta\nu_L\sqrt{1 + \frac{\Omega^2}{\Delta\nu_L}} \quad (4)$$

Here, $\Delta\nu_{\text{s}}$ is the saturated Lorentz width, $\Delta\nu_{\text{L}}$ is the unsaturated Lorentzian width and Ω is the Rabi frequency.

Inhomogeneous broadening

In inhomogeneous broadening, frequency shifts of absorbing particles differ from particle to particle. In a gas, the random distribution of particle velocities obeys Maxwell one. This is called Doppler broadening and its full width at half maximum is expressed as follows.

$$\Delta\nu_{\text{D}} = \frac{\sqrt{8k\ln 2}}{\lambda_0}\sqrt{\frac{T}{M}} \quad (5)$$

Here, k is the Boltamann constant, λ_0 is the center wave length of the absorption, M is the atomic weight of the absorbing atom and T is the translational temperature.

In this case, absorption saturation is more complex because the individual atoms are distinguishable. Then, the profile is an inhomogeneous profile in which each distinguishable part is homogeneous profile. The resulting profile is the convolution of homogeneous and inhomogeneous profiles as shown in Fig.4. This profile is called Voigt profile and absorption coefficient is expressed as follows.

$$k(\nu) = -\frac{\Delta N_0\lambda^2\Delta\nu_{\text{L}}}{16\pi^2 t_{\text{spont}}} \times\int_{-\infty}^{\infty}\frac{\exp[-\{2(\nu_\xi - \nu_0)/\Delta\nu_{\text{D}}\}^2\ln 2]d\nu_\xi}{(\nu-\nu_\xi) + (\Delta\nu_L/2)^2 + (\phi\lambda^2 I\Delta\nu_{\text{L}}/8\pi^2 h\nu)} \quad (6)$$

Here, ΔN_0 is the unsaturated population density and ν_0 is the center frequency of the inhomogeneous profile. Therefore, as for the broadening, the Doppler width is constant regardless of the laser intensity while the Lorentz width depends on it as in the homogeneous case.

If the Doppler broadening is much larger than Lorentz one, the Gaussian part in Eq. (6) can be pulled outside the integrand and the integral is calculated as follows.

$$k(\nu) = k_0(\nu)\left[1 + \frac{I}{I_{\text{s\_inhomo}}}\right]^{-1/2} \quad (7)$$

Here, $k_0(\nu)$ is the unsaturated absorption coefficient and obeys a Gauss profile. $I_{\text{s\_inhomo}}$ is the saturation intensity of inhomogeneous broadening and expressed as follows.

$$I_{\text{s\_inhomo}} = \frac{2\pi^2 h\nu\Delta\nu_{\text{L}}}{\phi\lambda^2} \quad (8)$$

The important difference between homogeneous and inhomogeneous cases is the frequency dependency of saturation intensity. The saturation intensity in inhomogeneous cases is independent of the line shape function g(ν). Therefore, the broadening of the profile remains constant, despite the variation of laser intensity. Since the area of Gauss profile is proportional to its center absorption coefficient and the broadening, the saturated and unsaturated integrated absorption coefficients K, K_0 have also the same relationship in Eq. (7), as follows.

$$K = K_0\left[1 + \frac{I}{I_{\text{s\_inhomo}}}\right]^{-1/2} \quad (9)$$

Experimental Setup

Glow Discharge Tube Measurement

The schematic of argon glow discharge tube experiments is shown in Fig.5. Tunable diode-lasers with an external cavity (DMD845, EOSI, and Velocity Model 6300, New Focus) were used as a laser oscillator. The modulation width and speed were 20 GHz and 10 Hz, respectively. An optical isolator is used to prevent the reflected laser beam from returning into the external cavity. The laser beam is divided into three beams by beam splitters. The first beam is directly detected by the photo-detector as a

reference signal. The second is detected by an ethalon, whose free spectral range is 0.75 GHz. The third is lead through the neutral density filters and the argon glow discharge tube whose input power is 3 mW and pressure is 79 Pa, and then detected by the photo-detector. By the combination of ND filters, the laser intensity can be changed from 0.58 mW/mm^2 to 3.8 μW/mm^2. The target lines are three argon atomic lines of 840.82 nm, 842.46 nm and 852.14 nm.

Arc-heater Measurement

The schematic of arc-heater experiments is shown in Fig.6. The optical system is almost the same as that of the discharge tube experiments. The difference is the probe laser beam. This beam is lead to the chamber window through a multimode optical fiber. The fiber output is mounted on a one-dimensional traverse stage to scan the plume in the radial directions. At the other side window, a parabola mirror is set and the laser beam is detected without synchronizing the detector position with the laser scan. Then, after the Abel inversion, the local absorption profiles are obtained. In this experiment, the laser intensity can be changed from 0.12 mW/mm^2 to 0.60 μW/mm^2 for the argon absorption laser and from 0.65 mW/mm^2 to 0.33 μW/mm^2 for the oxygen absorption laser. The argon target lines are the same as the discharge tube experiments and an oxygen target line is 777.19 nm. Table 1 shows these atomic lines data.

Table 1. ArI and OI transition data

	i	j	λ(nm)	E_i (eV)	E_j (eV)	g_i	g_j	$A_{ji}(10^7 s^{-1})$
ArI	$4s^2[1/2]$	$4p^2[3/2]$	840.82	11.8	13.3	3	5	2.23
ArI	$4s^2[3/2]$	$4p^2[5/2]$	842.46	11.6	13.1	3	5	2.15
ArI	$4s^2[1/2]$	$4p^2[3/2]$	852.14	11.8	13.3	3	3	1.39
OI	$3s^5S$	$3p^5P$	777.19	9.15	10.7	5	7	3.69

Results and Discussions

Glow Discharge Tube

Absorption profiles at 842.82 nm for various laser intensities are shown in Fig. 7. Since the best-fit Voigt parameter to the experimental profiles is up to 0.08, the Doppler broadening is assumed to be dominant and Lorentz one is neglected as shown in Eq (7). The result shows that the integrated absorption coefficient K and the Doppler width $\Delta\nu_D$ increase with the laser intensity. The maximum $\Delta\nu_D$ is 1.1 GHz at the laser intensity of 0.58 mW/mm^2 and the minimum one is 0.84 GHz at that of 3.8 μW/mm^2. As for the 840.82 nm and 852.14 nm profiles, the same tendency was obtained.

Figure 8 shows the measured K at 840.82 nm, 842.46 nm, and 852.14 nm profiles and the theoretical curves in Eq.(9) setting K_0 and I_s as fitting parameters. The measured values were well on the theoretical curves. The unsaturated population density calculated from these fitting of 840.82 nm and 852.14 nm are 1.07x10^{16} m^{-3} and 1.01x10^{16} m^{-3}, respectively. This result is quite reasonable because these absorption levels are same and the upper energy levels are also almost same. The I_s and $\Delta\nu_L$ are listed in Table 2. Here, the quenching rate ($Q/A_{ji} \approx 0$) in Eq. (7) has been neglected because of the low-pressure conditions.

Table 2 I_s and $\Delta\nu_L$

	840.82nm	842.46nm	852.14nm
I_s	0.146mW/mm^2	0.057mW/mm^2	0.271mW/mm^2
$\Delta\nu_L$	30.0MHz	11.7MHz	43.0MHz

Figure 9 shows translational temperature deduced from three argon lines, as a function normalized laser intensities. However, this result cannot be explained by the inhomogeneous saturation theory that the Doppler width is invariant for the change in the laser intensity.

To explain this result, it is assumed that the saturation intensity depends on the line shape function as the homogeneous case. Then, the I_s at every 0.1 GHz from the absorption center was calculated by fitting Eq. (7) to the absorption profiles of the various laser intensities as shown in Fig.7.

The obtained $1/I_s$ and the experimental absorption profile at the laser intensity of 3.8 μW/mm^2 are shown in Fig.10. These profiles are very similar with each other and their Gauss widths are 0.77 GHz and 0.86 GHz, respectively. Therefore, there may be a possibility that I_s in the inhomogeneous case is inversely proportional to the line shape function as the homogeneous case.

Arc-heater plume

Absorption profiles of ArI (842.82 nm) and OI (777.19 nm) after the Abel inversion for various laser intensities are shown in Figs.11 and 12. In this condition, the saturation has little been observed for the ArI profiles. Therefore, the saturation intensity of ArI was thought to be larger than that in the glow discharge tube plasma.

On the other hand, the saturation was observed for the OI profiles. Figure 13 shows the measured K of OI profiles for various laser intensities and the theoretical curve in Eq. (9), setting K_0 and I_s as fitting parameters. As a result, I_s and $\Delta\nu_L$ were found to be 0.22 mW/mm^2 and 25.9 MHz, respectively. As for the translational

temperature, however, it has been almost constant for any laser intensities as shown in Fig.14. This is because that in this case even the maximum I/I_s is up to unity. Then, in these experimental conditions, the Doppler width is not almost influenced by the saturation phenomena.

After all, it can be concluded that the difference between the translational temperatures deduced from two different species in our previous result is not originated from the saturation effect. Therefore, it is thought that there might be another broadening factor depending on species, otherwise the temperatures of different species might be originally different from each other.

Summary

In the glow discharge tube plasma, the strongly saturated profiles were observed at the laser intensity from 0.58 mW/mm^2 to 3.8 μW/mm^2.

Even in the inhomogeneous profile, the Doppler width increases with the laser intensity though this result contradicts the theory. This might be explained by the assumption that the saturation intensity in inhomogeneous profiles depends on the line shape function as the homogeneous case.

The difference between the translational temperatures deduced from two different species is not originated from the saturation effect.

Reference

1) Matsui, M. Komurasaki, K. and Arakawa, Y.: Laser Diagnostics of Atomic Oxygen in Arc-heater Plumes, AIAA paper 02-0793, 2002.

2) Matsui, M. Komurasaki, K. and Arakawa, Y.: Characterization of Arc-jet Type Arc-heater Plumes, AIAA paper 02-2242, 2002.

3) Bear, D.S. Hanson, R.K.: Semiconductor laser-based measurements of quench rates in an atmospheric pressure plasma by using saturated fluorescence spectroscopy, *App. Opt.* Vol. 32., No. 6, pp. 948-945. (1993)

4) Yariv, A.: *Quantum electronics*, New York, Wiley 2nd ed. (1975)

5) Davis, C.: Lasers and Electro-Optics, Cambridge, University press, 1996

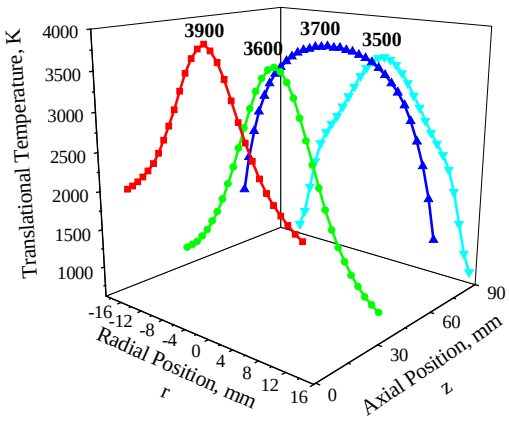

Fig. 1 Translational temperature distributions deduced from OI 777.19 nm line in arc-heater plumes.

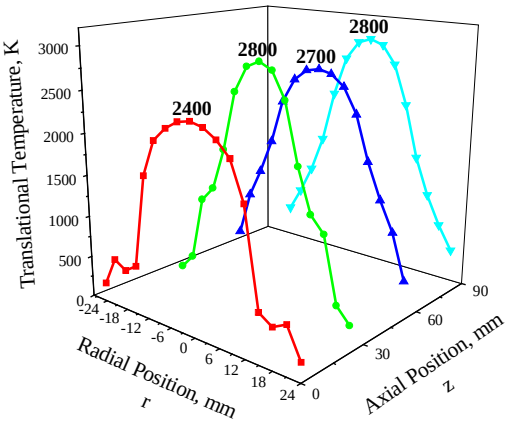

Fig. 2 Translational temperature distributions deduced from ArI 840.82 nm in arc-heater plumes.

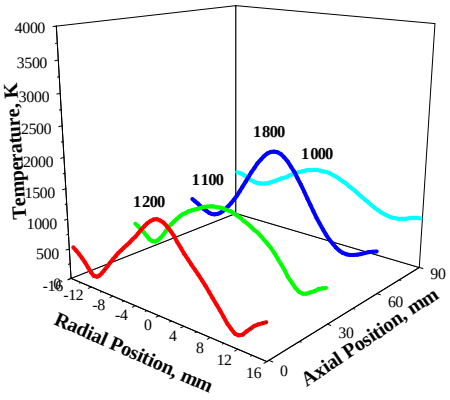

Fig.3 Translational temperature distributions calculated by a CFD analysis

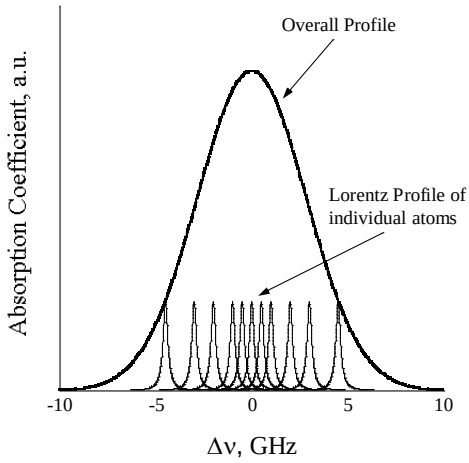

Fig. 4 Convolution of homogeneous and inhomogeneous profiles

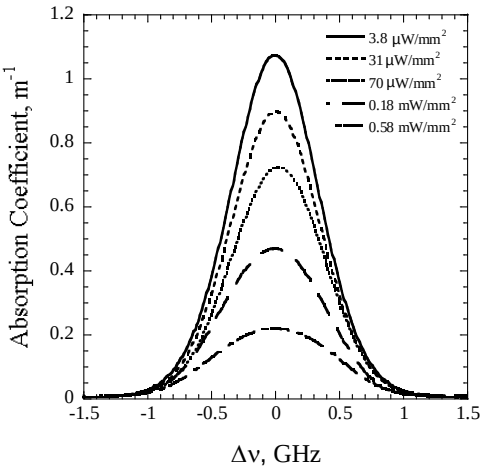

Fig. 7 Absorption profiles of 842.46nm for various laser intensities in glow discharge tube

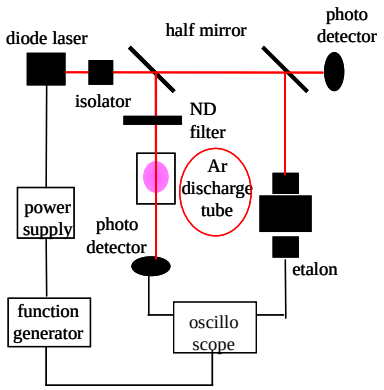

Fig. 5 Schematic of measurement system of argon discharge tube plasma

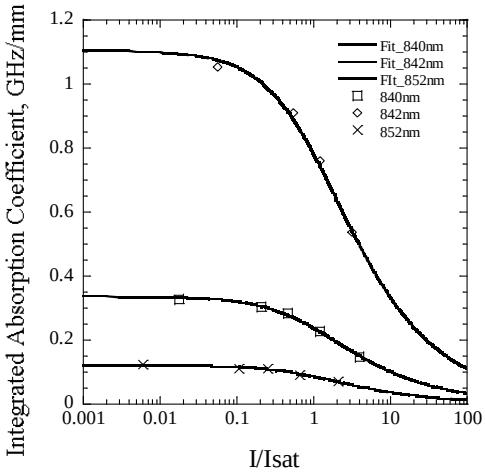

Fig. 8 ArI integrated absorption coefficients for different normalized laser intensity and curve fitting in glow discharge tube

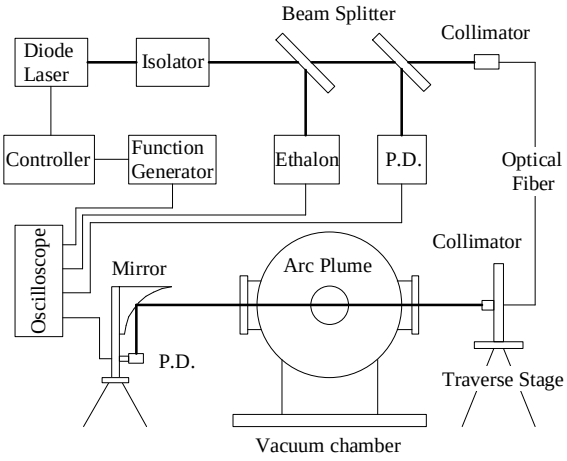

Fig. 6 Schematic of measurement system of the arc-heater plumes

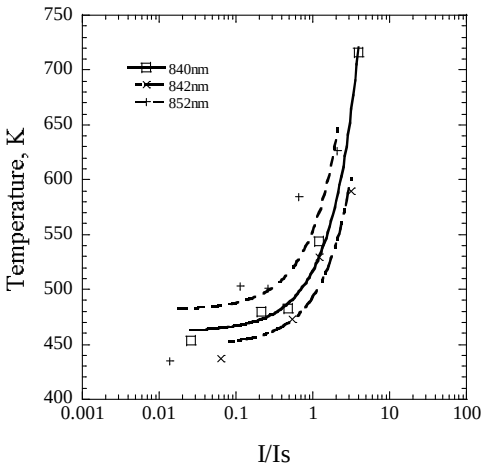

Fig. 9 Translational temperature deduced from ArI lines for various normalized laser intensity in glow discharge tube plasma

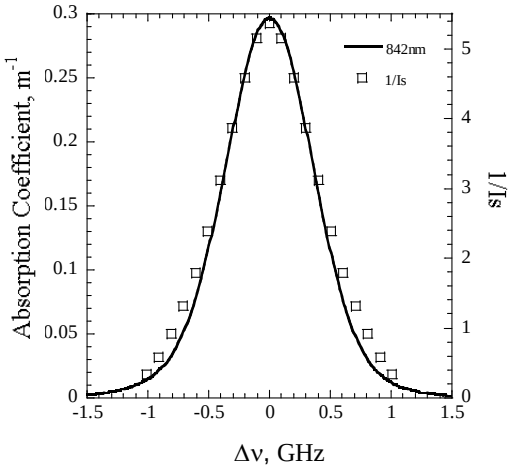

Fig. 10 Absorption profile at 840.82nm and $1/I_S$ profile

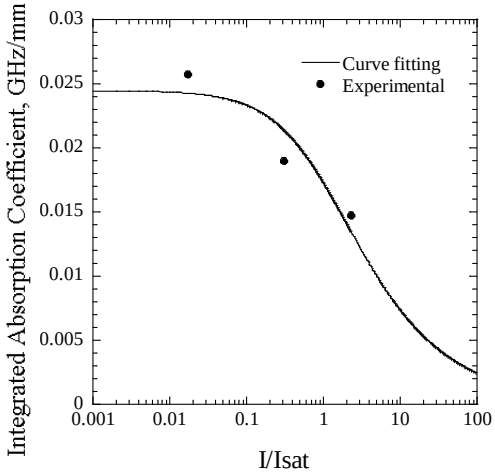

Fig. 13 OI integrated absorption coefficients for various normalized laser intensity and curve fitting in arc-heater plume

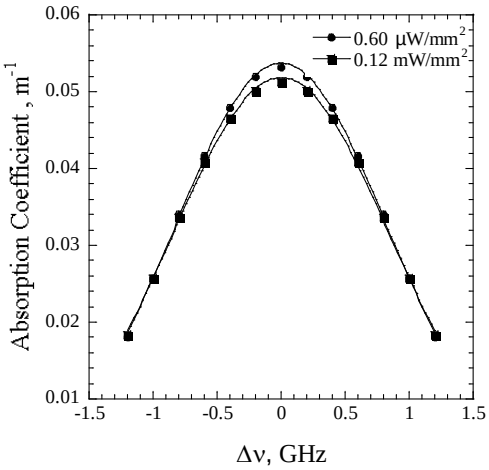

Fig. 11 Absorption profiles of ArI 842.46nm for various laser intensities in arc-heater plume

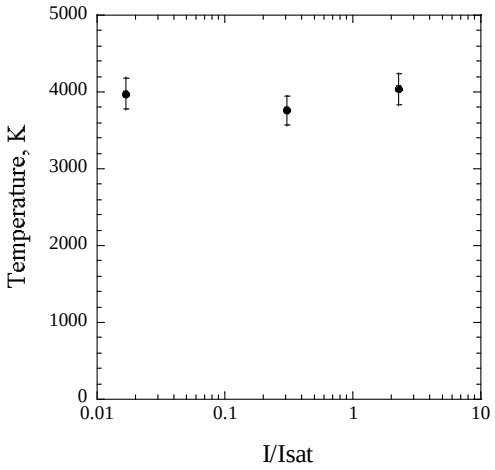

Fig. 14 Translational temperature deduced from OI line for various normalized laser intensity and curve fitting in arc-heater plume

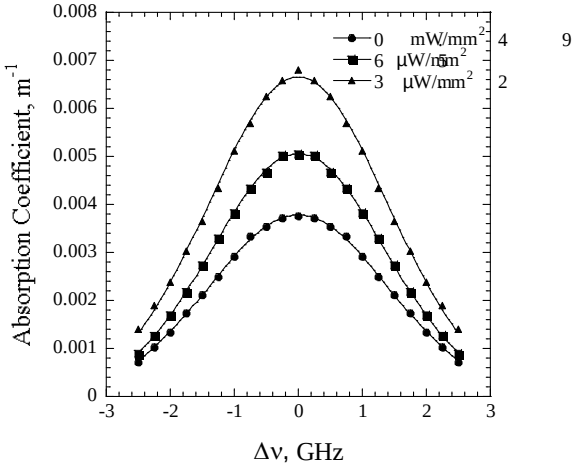

Fig. 12 Absorption profiles of OI 777.19nm for various laser intensities in arc-heater plume